Homogenization of a reaction-diffusion system modeling sulfate corrosion in locally-periodic perforated domains

Document status and date:
Published: 01/01/2009

Document Version:
Publisher's PDF, also known as Version of Record (includes final page, issue and volume numbers)

Please check the document version of this publication:

• A submitted manuscript is the version of the article upon submission and before peer-review. There can be important differences between the submitted version and the official published version of record. People interested in the research are advised to contact the author for the final version of the publication, or visit the DOI to the publisher's website.
• The final author version and the galley proof are versions of the publication after peer review.
• The final published version features the final layout of the paper including the volume, issue and page numbers.

Link to publication

Download date: 16. Nov. 2023

EINDHOVEN UNIVERSITY OF TECHNOLOGY
Department of Mathematics and Computer Science

Homogenization of a reaction-diffusion system modeling sulfate
corrosion in locally-periodic perforated domains

by

T. Fatima, N. Arab, E.P. Zemskov, A. Muntean

Homogenization of a reaction-diffusion system modeling sulfate corrosion in locally-periodic perforated domains

Tasnim Fatima (`t.fatima@tue.nl`)*
CASA - Centre for Analysis, Scientific computing and Applications, Department of Mathematics and Computer Science, Technical University Eindhoven, The Netherlands

Nasrin Arab (`nasrin.arab@gmail.com`)†
De Lismortel 246, 5612 AK Eindhoven, The Netherlands

Evgeny P. Zemskov (`zemskov@ccas.ru`)
Computing Centre of the Russian Academy of Sciences, Continuum Mechanics Department, Moscow, Russia

Adrian Muntean (`a.muntean@tue.nl`)
CASA - Centre for Analysis, Scientific computing and Applications, Department of Mathematics and Computer Science, Technical University Eindhoven, The Netherlands

Abstract. We discuss a reaction–diffusion system modeling concrete corrosion in sewer pipes. The system is coupled, semi-linear, and partially dissipative. It is defined on a *locally-periodic perforated domain* with nonlinear Robin-type boundary conditions at water-air and solid-water interfaces. We apply asymptotic homogenization techniques to obtain upscaled reaction–diffusion models together with explicit formulae for the effective transport and reaction coefficients. We show that the averaged system contains additional terms appearing due to the deviation of the assumed geometry from a purely periodic distribution of perforations for two relevant parameter regimes: (1) all diffusion coefficients are of order of $\mathcal{O}(1)$ and (2) all diffusion coefficients are of order of $\mathcal{O}(\varepsilon^2)$ except the one for $H_2S(g)$ which is of order of $\mathcal{O}(1)$. In case (1), we obtain a set of macroscopic equations, while in case (2) we are led to a two-scale model that captures the interplay between microstructural reaction effects and the macroscopic transport.

----

* Corresponding author
† Visiting CASA, Department of Mathematics and Computer Science, Technical University Eindhoven, The Netherlands

1. Introduction

Sulfuric acid is the cause of severe attack to concrete in sewerage systems. Although normally sewage does not affect the concrete matrix, under some conditions (like raised local temperature activating anaerobic bacteria of the species *Desulfovibrio desulfuricans*, e.g., and a suitable pH range) considerable production of hydrogen sulfide H_2S takes place and leads to acid attack [14]. This situation can be briefly described as follows: H_2S present in the air space of a sewer dissolves in stationary moisture films on the exposed concrete surfaces where it undergoes oxidation by aerobic bacteria to sulfuric acid. The chemical attack seem to take place only on the roof and upper part of the sewer where it finally leads to damage, i.e spalling of the material.

In spite of the fact that concrete has a long satisfactory service in sewarage systems, no hydraulic cement can withstand the acidity caused by the anaerobic conditions. In this paper, we focus our attention on forecasting the early stage of the corrosion[1].

We consider a semilinear reaction-diffusion system which we refer to as *micro-model*, see section 2.3 for the details. This describes the evolution of gaseous and dissolved H_2S, as well as of the sulfuric acid H_2SO_4, moisture, and gypsum at the pore level. Having as departure point a micro-model for this reaction-diffusion (RD) scenario, we want to derive, by means of asymptotic homogenization techniques, macroscopic RD models able to describe accurately the initiation of sulfate corrosion in sewer pipes. As further step, the "homogenized" models need to be tested against experimental findings at the macroscopic level and calibrated in order to forecast the penetration of the acid front.

A few basic questions are relevant at this stage:

(i) What would be "reasonable" assumptions which we may make concerning the microstructure of the concrete pipe? How much freedom we have for a deterministic averaging strategy?

(ii) Does the resulting macro-model approximate well the rather complex multi-scale physico-chemical situation?

(iii) How good is/can be this approximation?

---

[1] Whitish surface deposits appear, but the mechanical properties of the material stay unaffected. Note that at a later stage, a gradual softening of the cement paste appears and mechanical destabilization of the microstructure takes place. The literature reports about rates of corrosion of ca. 6–12 mm penetration depth per year.

Since the analysis we report here is only preliminary, we address particularly question (i) and leave questions (ii) and (iii) for the moment unanswered.

The paper is organized as follows: In section 2 we give a minimal modeling at the pore level of the relevant physicochemical processes involved in the early stage of sulfate corrosion of cement-based materials and explain both the flexibility and limitations of our modeling. We define in section 2.1 a periodic-cells approximation of the part of the concrete pipe we are looking at as well as the corresponding locally-periodic array of perforations. We nondimensionalize in section 3 the micro-model presented in section 2.3. The homogenization procedure, the macro and micro-macro mass-balance equations together with a list of effective transport and reaction coefficients are presented in section 4.

A FEW COMMENTS ON RELATED LITERATURE

The reader can find details on civil engineering aspects concerning concrete corrosion issues when acid attack is involved, for instance, in [4, 3, 27, 25, 19, 29]. We particularly like [4] for the clear exposition of the phenomenology and for the enumeration of the main mechanisms influencing acid corrosion. A standard reference work concerning cement chemistry is [28].

From the modeling point of view, we were very much inpired by [7] [see also the subsequent papers [17, 18]], where the authors adopted a macroscopic moving-boundary modeling strategy to capture the macroscopic corrosion front penetrating the pipe. We adapted some of their modeling ideas for the micro-model proposed in section 2.3. Another macroscopic approach for a closely related sulfatation problem has been reported in [1].

At the technical level, we essentially use formal asymptotics techniques for both the periodic and locally-periodic homogenization. We refer the reader to [2] for a discussion on uniform descriptions of heterogeneous media, while the working technique is detailed for instance in [6, 26], and [11] (chapter 7); see also [30] for a related application. Refs. [9, 15, 20, 11] contain more theoretical approaches able to justify the asymptotics at least for simpler PDE models.

Homogenization problems in *locally-periodic perforated domains* have been dealt with in [21, 5, 8, 9], e.g.; see [10] for a more recent account of bibliographic information. At the technical level, we rely on the analysis reported in [8] for the case of a Poisson problem with a linear Fourier condition imposed at the boundary of the perforation. We assume a locally-periodic distribution of the perforations (i.e. of

the micropores). By this we step away from the often used periodic approximation of porous media, which for the particular case of concrete is much too rough. Moreover, we expect that some randomness is needed for better covering what happens in reality, but we prefer for the moment to stick with a deterministic approach and understand [for this easier case] the occurrence of new terms expressing deviations from periodicity.

Structured transport in porous media, like that arising when gaseous and dissolved chemical species (here: $H_2S(g)$ and $H_2S(aq)$) diffuse simultaneously, multi-spatial-scale situations naturally occur [12, 22, 23, 24]. Many of these models can be derived rigorously by means of homogenization techniques [16]. Note that the formal analysis done for a two-scale setting in section 3.3.2 of [22] remotely ressembles ours for the case (2).

2. Modeling sulfate corrosion in sewer pipes

In this section, we describe the geometry of the sewer and present our concept of microstructure. Next we recall the physical and chemical mechanisms that we take into account, and finally, we list the equations entering our micro-model.

2.1. Description of the problem and geometry

We consider a cross-section of a sewerage pipe made of partially wet concrete. It is worth noting that concrete is a mixture of cement, gel and mobile water as well as of aggregate (sand, gravels, etc). Therefore we assume that any microstructure (any representative cell) contains three non-overlapping regions: the solid matrix (aggregate, eventually inaccessible-to-diffusion gel water, cement paste, etc.), the pore water clinging on solid fabrics as well as the air-filled part of the pore; see Fig. 1 for a sketch of the cell geometry, say Y, divided into three (distinct and non-mixed) components: solid, water, and air. We assume that the solid part is placed in the center of the cell which is enclosed by a stationary water film. Around the water film, we assume the presence of bulk air as shown in Fig 1 (bottom). Additionally, we assume that the domain of interest can be approximated by a finite union of this kind of cells.

Let us now have a look on our perforations: Each cell contains two internal interfaces: one separating the solid part from the water film, and the second separating the water film from the air part. We consider the following constraints to be fulfilled:
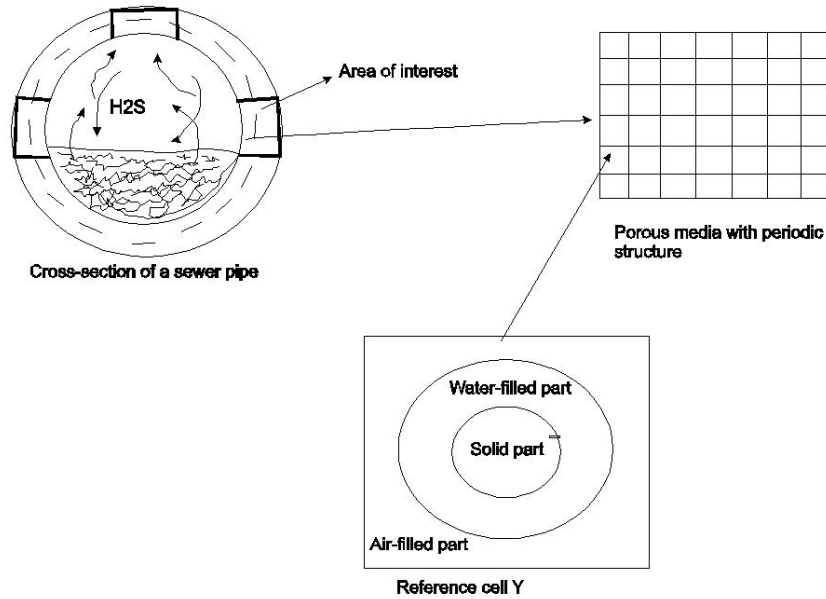
Figure 1. Top left: Cross section of a sewer showing 3 critical regions where corrosion initiates; Top right: Periodic grid covering one of the critical regions; Bottom: Typical pore/reference cell.

(i) Each cell contains all three regions: solid, air, and water. None of them disappears during the RD process. The shapes of their outer boundaries do not evolve with the time[2], but are allowed to be x-dependent. This means that they may be *different* at different space positions.

(ii) The x-dependency of the internal interfaces mentioned in (i) is *locally periodic*.

(iii) All internal interfaces are sufficiently smooth.

   Usually, in periodic homogenization approaches (like in [6, 11]) the shape of these interfaces (i.e. the boundary of the perforations) is x-independent. If the shape of the internal interfaces in the cell is not x-dependent, then the outer normals to these interfaces depend on the fast variable $y = \frac{x}{\epsilon}$ only. Hence, oscillations of the internal boundaries from cell to cell cannot be captured anymore.

_____

[2] Ref. [31] reports about a homogenization procedure which can deal (unfortunately only) formally with evolving microstructures for a precipitation/dissolution problem.

We notice in section 4 that the dependence of the normals vectors to the active internal interfaces on both x and y variables involves difficulties at the technical level, but the fact that (ii) holds will be very helpful in controlling (at least formally) the oscillations.

2.2. NOTATION

Let Ω be an open set in $\mathbb{R}^3$ with a smooth boundary Γ having two disjoint pieces Γ^D and Γ^N. Here $\Gamma^D \cup \Gamma^N = \Gamma$ and $\mu(\Gamma^D) \neq 0$, where μ is the (surface) Lebesque measure in $\mathbb{R}^2$. The domain Y is the reference cell in $\mathbb{R}^3$, while $S := (0, T)$ is the time interval. Y splits up into Y^a - the air-filled part of the cell, Y^w - the water-filled part of the cell, and Y^s - solid part of the cell. Furthermore,

$$Y := Y^w \cup Y^s \cup Y^a \text{ with } Y^w \cap Y^s \cap Y^a = \emptyset.$$

Also, we denote $\Gamma^{sw} := \partial Y^s$ to be the interface between water and solid part of the cell and $\Gamma^{wa} := \partial Y^w$ as the interface between the water-filled and air-filled part of the cell.

2.2.1. *Periodic array of perforations*
For a subset X of Y and the integer vectors $k = (k_1, k_2, k_3) \in \mathbb{Z}^3$, we denote the shifted subset by

$$X_k := X + \sum_{i=1}^{3} k_i e_i, \tag{1}$$

where e_i is the ith unit vector in $\mathbb{R}^3$.

We assume that $\hat{\Omega}_\varepsilon$ is made up of copies of the unit cell scaled by a sufficiently small scaling factor $\varepsilon > 0$. Here ε is a small parameter whose precise meaning will become clear in section 3.

$\hat{\Omega}_\varepsilon := \hat{Y}_\varepsilon^a \cup \hat{Y}_\varepsilon^w \cup \hat{Y}_\varepsilon^s$;

$\hat{Y}_\varepsilon^a := \bigcup_{k \in \mathbb{Z}^3} \{\varepsilon Y_k^a | \varepsilon Y_k^a \subset \Omega\}$, the air-filled part of the pores;

$\hat{Y}_\varepsilon^w := \bigcup_{k \in \mathbb{Z}^3} \{\varepsilon Y_k^w | \varepsilon Y_k^w \subset \Omega\}$, the water-filled part of the pores;

$\hat{Y}_\varepsilon^s := \bigcup_{k \in \mathbb{Z}^3} \{\varepsilon Y_k^s | \varepsilon Y_k^s \subset \Omega\}$, solid matrix;

$\hat{\Gamma}_\varepsilon^{sw} := \bigcup_{k \varepsilon Z^n} \{\varepsilon \Gamma_k^{sw} | \varepsilon \Gamma_k^{sw} \subset \Omega\}$ water-solid interface;

$\hat{\Gamma}_\varepsilon^{wa} := \bigcup_{k \varepsilon Z^n} \{\varepsilon \Gamma_k^{wa} | \varepsilon \Gamma_k^{wa} \subset \Omega\}$ water-air interface.

2.2.2. *Locally-periodic array of perforations*
In the locally-periodic setting, one represents the normal vector n^ε to the "oscillating" internal boundaries of the perforations in the form suggested, for instance, in [9, 5]:

$$n^\varepsilon(x, y) := \tilde{n}(x, y) + \varepsilon n'(x, y) + \mathcal{O}(\varepsilon^2), \tag{2}$$

where

$$\tilde{n}(x,y) = \frac{\nabla_y P(x,y)}{|\nabla_y P(x,y)|} \tag{3}$$

and

$$n'(x,y) = \frac{\nabla_x P(x,y)}{|\nabla_y P(x,y)|} - \nabla_y P(x,y) \frac{\nabla_x P(x,y), \nabla_y P(x,y)}{|\nabla_y P(x,y)|^3}. \tag{4}$$

Here the generic surface $P(x,y)$, which describes the interfaces[3] Γ_ε^{sw}, Γ_ε^{wa}, and Γ_ε, respectively, is assumed to be 1-periodic function in the variable y and sufficiently smooth with respect to both variables x, y.

It is worth noting that for uniformly periodic perforations $\tilde{n}$ only depends in y and $n' = 0$. To give a meaning to the formal calculations, which we perform in this paper, is enough to define the locally-periodicity appearing in the geometry from 2 (left) using the description (2) of the normal vectors to the non-periodically-placed interfaces.
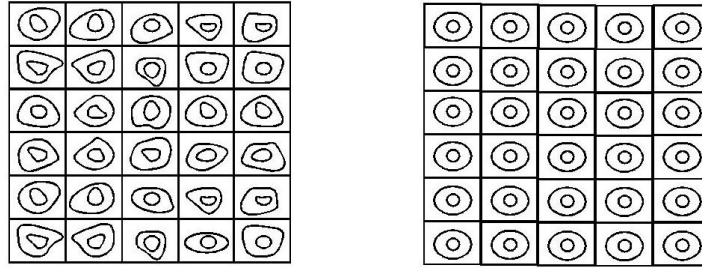
Figure 2. Left: Locally periodic array of perforations; Right: Uniformly periodic array of perforations. In the two pictures, we expect the occurrence of differences at most of order of $\mathcal{O}(\varepsilon)$ between any two corresponding inner interfaces .

We refer the reader to [5] for an accurate mathematical description of the geometry described in Figure 2 (left) and to [21] for connections between locally-periodic perforated domains and quasi-periodic functions. See [15] for a notation strategy for the periodic case.

2.3. Micro-model

List of data and unknowns

The data is given by

$u_{10} : \Omega \longrightarrow \mathbb{R}_+$ - the initial concentration of $H_2SO_4(aq)$

---

[3] Γ_ε^{sw}, Γ_ε^{wa}, and Γ_ε point out the same class of objects as those defined in the periodic setting with the same name under a hat, but now the periodicity assumption is removed. The same statment holds for Ω_ε, Y_ε^a, Y_ε^w, and Y_ε^s.

$u_{20} : \Omega \longrightarrow \mathbb{R}_+$ - the initial concentration of $H_2S(aq)$

$u_{30} : \Omega \longrightarrow \mathbb{R}_+$ - the initial concentration of $H_2S(g)$

$u_{40} : \Omega \longrightarrow \mathbb{R}_+$ - the initial concentration of dissolved gypsum

$u_{50} : \Omega \longrightarrow \mathbb{R}_+$ - the initial concentration of moisture

$u_3^D : \Gamma_D \times S \longrightarrow \mathbb{R}_+$ - exterior concentration (Dirichlet data) of $H_2S(g)$

The unknowns are

$u_1^\varepsilon : Y_\varepsilon^w \times S \longrightarrow \mathbb{R}$ - mass concentration of $H_2SO_4(aq)$ $[g/cm^3]$

$u_2^\varepsilon : Y_\varepsilon^w \times S \longrightarrow \mathbb{R}$ - mass concentration of $H_2S(aq)$ $[g/cm^3]$

$u_3^\varepsilon : Y_\varepsilon^a \times S \longrightarrow \mathbb{R}$ - mass concentration of $H_2S(g)$ $[g/cm^3]$

$u_4^\varepsilon : Y_\varepsilon^w \times S \longrightarrow \mathbb{R}$ - mass concentration of moisture $[g/cm^3]$

$u_5^\varepsilon : \Gamma_\varepsilon^{sw} \times S \longrightarrow \mathbb{R}$ - mass concentration of gypsum $[g/cm^2]$

The mass-balance equation for $H_2(SO)_4$ is

$$
\begin{array}{rcl}
\partial_t u_1^\varepsilon + div(-d_1^\varepsilon \nabla u_1^\varepsilon) & = & -k_1^\varepsilon u_1^\varepsilon + k_2^\varepsilon u_2^\varepsilon, \quad x \in Y_\varepsilon^w, t \in S \\
u_1^\varepsilon(x,0) & = & u_{10}^\varepsilon(x), \quad x \in Y_\varepsilon^w \\
n^\varepsilon \cdot (-d_1^\varepsilon \nabla u_1^\varepsilon) & = & 0, \quad x \in \Gamma_\varepsilon^{wa}, t \in S \\
n^\varepsilon \cdot (-d_1^\varepsilon \nabla u_1^\varepsilon) & = & -\eta(u_1^\varepsilon, u_5^\varepsilon), \quad x \in \Gamma_\varepsilon^{sw}, t \in S
\end{array}
\tag{5}
$$

The mass-balance equation for $H_2S(aq)$ is given by

$$
\begin{array}{rcl}
\partial_t u_2^\varepsilon + div(-d_2^\varepsilon \nabla u_2^\varepsilon) & = & k_1^\varepsilon u_1^\varepsilon - k_2^\varepsilon u_2^\varepsilon, \quad x \in Y_\varepsilon^w, t \in S \\
u_2^\varepsilon(x,0) & = & u_{20}^\varepsilon(x), \quad x \in Y_\varepsilon^w \\
n^\varepsilon \cdot (-d_2^\varepsilon \nabla u_2^\varepsilon) & = & \varepsilon(a^\varepsilon(x)u_3^\varepsilon - b^\varepsilon(x)u_2^\varepsilon), \quad x \in \Gamma_\varepsilon^{wa}, t \in S \\
n^\varepsilon \cdot (-d_2^\varepsilon \nabla u_2^\varepsilon) & = & 0, \quad x \in \Gamma_\varepsilon^{sw}, t \in S
\end{array}
\tag{6}
$$

The mass-balance equation for $H_2S(g)$ is given by

$$
\begin{array}{rcl}
\partial_t u_3^\varepsilon + div(-d_3^\varepsilon \nabla u_3^\varepsilon) & = & 0, \quad x \in Y_\varepsilon^a, t \in S \\
u_3^\varepsilon(x,0) & = & u_{30}^\varepsilon(x), \quad x \in Y_\varepsilon^a \\
n^\varepsilon \cdot (-d_3^\varepsilon \nabla u_3^\varepsilon) & = & 0, \quad x \in \Gamma^N, t \in S \\
u_3^\varepsilon(x,t) & = & u_3^D(x,t), \quad x \in \Gamma^D, t \in S \\
n^\varepsilon \cdot (-d_3^\varepsilon \nabla u_3^\varepsilon) & = & -\varepsilon(a^\varepsilon(x)u_3^\varepsilon - b^\varepsilon(x)u_2^\varepsilon), \quad x \in \Gamma_\varepsilon^{wa}, t \in S
\end{array}
\tag{7}
$$

The mass-balance equation for moisture is given by

$$
\begin{array}{rcl}
\partial_t u_4^\varepsilon + div(-d_4^\varepsilon \nabla u_4^\varepsilon) & = & k_1^\varepsilon u_1^\varepsilon, \quad x \in Y_\varepsilon^w, t \in S \\
u_4^\varepsilon(x,0) & = & u_{40}^\varepsilon(x), \quad x \in Y_\varepsilon^w \\
n^\varepsilon \cdot (-d_4^\varepsilon \nabla u_4^\varepsilon) & = & 0, \quad x \in \Gamma_\varepsilon^{wa}, t \in S \\
n^\varepsilon \cdot (-d_4^\varepsilon \nabla u_4^\varepsilon) & = & 0, \quad x \in \Gamma_\varepsilon^{sw}, t \in S
\end{array}
\tag{8}
$$

The mass-balance equation for the gypsum present at the water-solid interface is

$$
\begin{array}{rcl}
\partial_t u_5^\varepsilon & = & \eta(u_1^\varepsilon, u_5^\varepsilon), \quad x \in \Gamma_\varepsilon^{sw}, t \in S \\
u_5^\varepsilon(x,0) & = & u_{50}^\varepsilon(x), \quad x \in \Gamma_\varepsilon^{sw}.
\end{array}
\tag{9}
$$

Note that the lack of diffusion in (9) gives the partly dissipative feature to the model.

The list of coefficients in (5)-(9) is as follows:

$k_j^\varepsilon : \Omega \times S \longrightarrow \mathbb{R}$ - reaction constants for all $j \in \{1, 2, 3\}$,

$d_i^\varepsilon : \Omega \times S \longrightarrow \mathbb{R}^{3 \times 3}$ - diffusion coefficients for H_2SO_4, $H_2S(aq)$, $H_2S(g)$ and H_2O for all $i \in \{1, 2, 3, 4\}$,

$a^\varepsilon : \Gamma_\varepsilon^{wa} \times S \longrightarrow \mathbb{R}$ - the adsorption factor of H_2S (air to water),

$b^\varepsilon : \Gamma_\varepsilon^{wa} \times S \longrightarrow \mathbb{R}$ - the desorption factor of H_2S (air to water),

$\eta : \Gamma_\varepsilon^{sw} \times S \longrightarrow \mathbb{R}$ - reaction rate on water-solid interface.

It is tacitly assumed that all reaction constants, diffusion coefficients, absorption and desorption factors as well as normal vectors to the water-solid and water-air interfaces are Y-periodic functions as follows: $d_i^\varepsilon(x, t) := d_i(\frac{x}{\varepsilon}, t)$, $i \in \{1, 2, 3, 4\}$, $k_j^\varepsilon(x, t) := k_j(\frac{x}{\varepsilon}, t)$, $j \in \{1, 2, 3\}$; $a^\varepsilon(x, t) := a(\frac{x}{\varepsilon}, t)$, and $b^\varepsilon(x, t) := b(\frac{x}{\varepsilon}, t)$.

To fix ideas, notice that the reaction rate η may take the form

$$\eta(\alpha, \beta) = \begin{cases} k_3^\varepsilon(x) \alpha^p (\bar{c} - \beta)^q, & \text{if } \alpha \geq 0, \beta \geq 0 \\ 0, & \text{otherwise} \end{cases}$$

where $\bar{c}$ is a known constant. The reader is referred to [7, 29] for more modeling details.

Note that the micro-model can be easily extended by allowing for ionic transport and the reaction of sulfate ions with the aluminate phases in concrete. A much more difficult step is to model the reaction-induced deformation of the microstructure and to account for the simultaneous space- and time-evolution of the active parts of the perforations.

3. Nondimensionalization

We introduce the characteristic length L for the space variable such that $x = L\tilde{x}$, the time variable is scaled as $t = \tau s$, and for the concentrations we use $u_i^\varepsilon = u_{ref}^i v_i^\varepsilon$, where[4] $u_{ref}^i = \|u_i^\varepsilon\|_\infty$ for all $i \in \{1, 2, 3, 4, 5\}$. k_j are scaled as $k_j^\varepsilon = k_j^* \tilde{k}_j^\varepsilon$, where $k_j^* = \| k_j^\varepsilon \|_\infty$ for all $j \in \{1, 2, 3\}$ and $d_i := d_{ref}^i \tilde{d}_i$ for all $i \in \{1, 2, 3, 4\}$. We make use of two mass-transfer Biot numbers[5] for the two spatial scales in question: *micro* and *macro*.

---

[4] L^∞-bounds on concentrations and the existence of positive weak solutions to the micro-model are shown in [13].

[5] Biot numbers are dimensionless quantities mostly used in heat transfer calculations. They relate the heat transfer (mass transfer) resistance inside and at the surface of a body.

Our first Biot number is defined by

$$Bi^m := \frac{b_{ref}^m L}{\mathfrak{D}}, \tag{10}$$

where b_{ref}^m is a reference reaction rate acting at the water solid interface within the microstructure and $\mathfrak{D}$ is a reference diffusion coefficient. Our second Biot number is defined by

$$Bi^M := \frac{b_{ref}^M L}{\mathfrak{D}}, \tag{11}$$

where b_{ref}^M is a reference reaction rate at the water-solid interface at the macro level. The connection between the two Biot numbers is given by

$$Bi^m = \varepsilon Bi^M. \tag{12}$$

In some sense, relation (12) defines our small scaling parameter ε with respect to which we wish to homogenize. Furthermore, we introduce two other dimensionless numbers:

$$\beta_i := \frac{u_{ref}^i}{u_{ref}^1} \text{ and } \gamma_i := \frac{d_{ref}^i}{d_{ref}^3}. \tag{13}$$

β_i represents the ratio of the maximum concentration of the ith species to the maximum H_2SO_4 concentration, while γ_i denotes the ratio of the characteristic time of the ith diffusive aqueous species to the characteristic diffusion time of $H_2S(g)$.

In terms of the newly introduced quantities, the mass-balance equation for H_2SO_4 takes the form

$$\frac{u_{ref}^1}{\tau} \partial_s v_1^\varepsilon + \frac{u_{ref}^1 d_{ref}^1}{L^2} div(-\tilde{d}_1 \nabla v_1^\varepsilon) = -k_1^* u_{ref}^1 \tilde{k}_1^\varepsilon v_1^\varepsilon + k_2^* u_{ref}^2 \tilde{k}_2^\varepsilon v_2^\varepsilon, \tag{14}$$

and hence,

$$\beta_1 \partial_s v_1^\varepsilon + \frac{\beta_1 d_{ref}^1 \tau}{L^2} div(-\tilde{d}_1 \nabla v_1^\varepsilon) = -\frac{k_1^* u_{ref}^1 \tau}{u_{ref}^1} \tilde{k}_1^\varepsilon v_1^\varepsilon + \frac{k_2^* u_{ref}^2 \tau}{u_{ref}^1} \tilde{k}_2^\varepsilon v_2^\varepsilon. \tag{15}$$

As reference time, we choose the characteristic time scale of the fastest species (here: $H_2S(g)$), that is $\tau := \tau_{diff} = \frac{L^2}{d_{ref}^3}$. We get

$$\beta_1 \partial_s v_1^\varepsilon + \beta_1 \gamma_1 div(-\tilde{d}_1 \nabla v_1^\varepsilon) = -\frac{\eta_{ref}^1 \tau}{u_{ref}^1} \tilde{k}_1^\varepsilon v_1^\varepsilon + \frac{\eta_{ref}^2 \tau}{u_{ref}^1} \tilde{k}_2^\varepsilon v_2^\varepsilon \tag{16}$$

Let us denote by $\tau_{reac}^j := \frac{u_{ref}^1}{\eta_{ref}^j}$ the characteristic time scale of the jth reaction, where the quantity η_{ref}^j is a reference reaction rate for the

corresponding chemical reaction. With this new notation in hand, we obtain

$$\beta_1 \partial_s v_1^\varepsilon + \beta_1 \gamma_1 div(-\tilde{d}_1 \nabla v_1^\varepsilon) = -\Phi_1^2 \tilde{k}_1^\varepsilon v_1^\varepsilon + \Phi_2^2 \tilde{k}_2^\varepsilon v_2^\varepsilon \tag{17}$$

where $\Phi_j^2, j \in \{1, 2, 3\}$ are Thiele-like moduli. The jth Thiele modulus Φ_j^2 compares the characteristic time of the diffusion of the fastest species and the characteristic time of the jth chemical reaction. It is defined as

$$\Phi_j^2 := \frac{\tau_{diff}}{\tau_{reac}^j} \text{ for all } j \in \{1, 2, 3\}. \tag{18}$$

For the boundary condition involving a surface reaction, we obtain

$$\tilde{n}_\varepsilon \cdot (-\tilde{d}_1 \nabla v_1^\varepsilon)) = -\frac{\tau_{diff}}{\gamma_1 L \tau_{reac}^3} \tilde{\eta}(v_1^\varepsilon, v_5^\varepsilon), \tag{19}$$

and therefore,

$$\tilde{n}_\varepsilon \cdot (-\tilde{d}_1 \nabla v_1^\varepsilon)) = -\varepsilon \frac{\Phi_3^2}{\gamma_1} \tilde{\eta}(v_1^\varepsilon, v_5^\varepsilon). \tag{20}$$

Note that the quantity $\varepsilon \Phi_3^2$ plays the role of a Thiele modulus for a surface reaction, while Φ_1^2 and Φ_2^2 are Thiele moduli for volume reactions. Similarly, the mass-balance equation for the species $H_2S(aq)$ becomes

$$\beta_2 \partial_s v_2^\varepsilon + \beta_2 \gamma_2 div(-\tilde{d}_2 \nabla v_2^\varepsilon) = \Phi_1^2 \tilde{k}_i v_1^\varepsilon - \Phi_2^2 \tilde{k}_2 v_2^\varepsilon. \tag{21}$$

The boundary condition at the air-water interface becomes

$$\tilde{n}_\varepsilon \cdot (-\tilde{d}_2 \nabla v_2^\varepsilon)) = \varepsilon Bi^M (\frac{a^\varepsilon \beta_3}{b^\varepsilon \beta_2} v_3^\varepsilon - v_2^\varepsilon). \tag{22}$$

The mass balance equation for $H_2S(g)$ is

$$\beta_3 \partial_s v_3^\varepsilon + \beta_3 div(-\tilde{d}_3 \nabla v_3^\varepsilon) = 0, \tag{23}$$

while the boundary condition at the air-water interface reads

$$\tilde{n}_\varepsilon \cdot (-\tilde{d}_3 \nabla v_3^\varepsilon)) = -\varepsilon Bi^M (\frac{a^\varepsilon}{b^\varepsilon} v_3^\varepsilon - \frac{\beta_2}{\beta_3} v_2^\varepsilon). \tag{24}$$

Finally, the mass-balance equation for moisture is

$$\beta_4 \partial_s v_4^\varepsilon + \beta_4 \gamma_4 div(-\tilde{d}_4 \nabla v_4^\varepsilon) = \Phi_1^2 \tilde{k}_1 v_1^\varepsilon \tag{25}$$

and the ODE for gypsum becomes

$$\beta_5 \partial_s v_5^\varepsilon = \Phi_3^2 \tilde{\eta}(v_1^\varepsilon, v_5^\varepsilon). \tag{26}$$

To simplify the notation, we drop all the tildes and keep the meaning of the unknowns and operators as mentioned in this section.

4. Formal homogenization procedure

Homogenization is a generic term which refers to finding *effective* model equations and coefficients, i.e. objects independent of ε. For our problem, the homogenization procedure will provide us an approximate macroscopic model (that we refer to as macro-model) defined for a uniform medium, where the original microstructure and phase separation (water, air, and solid) can not be seen anymore. The hope is that the solutions to the macro-model are sufficient close[6] to the solutions of the micro-model as ε goes to zero.

In this section, we study the asymptotic behaviour of the solutions to the micro-model as $\varepsilon \to 0$ for two parameter regimes reflecting two different types of diffusive-like transport of chemical species in concrete: "uniform" diffusion (see section 4.1) and "structured" diffusion (section 4.2).

4.1. Case 1: $d_i^\varepsilon = \mathcal{O}(1)$ for all $i \in \{1, 2, 3, 4\}$

We consider that the diffusion speed is comparable for all concentrations, i.e. the diffusion coefficients d_i^ε are of order of $\mathcal{O}(1)$ w.r.t. ε for all $i \in \{1, 2, 3, 4\}$. We assume that the solutions $v_i^\varepsilon(x, t)$ ($i \in \{1, 2, 3, 4, 5\}$) of the micro-model admit the following asymptotic expansion

$$v_i^\varepsilon(x, t) = v_{i0}(x, y, t) + \varepsilon v_{i1}(x, y, t) + \varepsilon^2 v_{i2}(x, y, t) + \dots, \qquad (27)$$

where $y = \frac{x}{\varepsilon}$ and the functions $v_{im}(x, y, t), m = 1, 2, 3, \dots$, are Y-periodic in y.

If we define (compare [6, 11], e.g.)

$$\Psi_\varepsilon(x, t) := \Psi(x, \frac{x}{\varepsilon}, t),$$

then

$$\frac{\partial \Psi_\varepsilon}{\partial x_i} = \frac{\partial \Psi}{\partial x_i}(x, \frac{x}{\varepsilon}) + \frac{1}{\varepsilon}\frac{\partial \Psi}{\partial y_i}(x, \frac{x}{\varepsilon}) \qquad (28)$$

We investigate the asymptotic behavior of the solution $v_1^\varepsilon(x, t)$ as $\varepsilon \to 0$ of the following problem posed in the domain Y_ε^w

$$\begin{aligned}
\beta_1 \partial_s v_1^\varepsilon + \beta_1 \gamma_1 div(-d_1 \nabla v_1^\varepsilon) &= -\Phi_1^2 k_1^\varepsilon v_1^\varepsilon + \Phi_2^2 k_2^\varepsilon v_2^\varepsilon \text{ in } Y_\varepsilon^w, \\
v_1^\varepsilon(x, t) &= 0 \text{ 0n } \Gamma, \\
n_\varepsilon \cdot (-d_1 \nabla v_1^\varepsilon)) &= -\varepsilon \frac{\Phi_3^2}{\gamma_1} \eta(v_1^\varepsilon, v_5^\varepsilon) \text{ on } \Gamma_\varepsilon^{sw}, \\
n_\varepsilon \cdot (-d_1 \nabla v_1^\varepsilon)) &= 0 \text{ on } \Gamma_\varepsilon^{wa},
\end{aligned} \qquad (29)$$

---

[6] The status of being "close" needs rigorous concepts (and proofs) that will be discussed in a forthcoming paper.

Using now the asymptotic expansion of the solution $v_1^\varepsilon(x,t)$ in (29) and equating the terms with the same powers of ε, we obtain:

$$\begin{cases} A_0 v_{10} = 0 \ \ \text{in} \ \ Y_\varepsilon^w, \\ v_{10} \ \ \text{Y-periodic in} \ \ y, \end{cases} \tag{30}$$

where the operator A_0 is given by

$$A_0 := -\sum_{i,j=1}^3 \frac{\partial}{\partial y_i}\left(d_1^{ij}\frac{\partial}{\partial y_j}\right).$$

As next step, we get

$$\begin{cases} A_0 v_{11} = -A_1 v_{10} \ \ \text{in} \ \ Y_\varepsilon^w, \\ v_{11} \ \ Y - periodic \ \ \text{in} \ \ y, \\ (d_1\nabla_y v_{11}, \tilde{n}) = -(d_1\nabla_x v_{10}, \tilde{n}), \end{cases} \tag{31}$$

where

$$A_1 := -\sum_{i,j=1}^3 \frac{\partial}{\partial x_i}\left(d_1^{ij}\frac{\partial}{\partial y_j}\right) - \sum_{i,j=1}^3 \frac{\partial}{\partial y_i}\left(d_1^{ij}\frac{\partial}{\partial x_j}\right).$$

Furthermore, it holds that

$$\begin{aligned} \beta_1\gamma_1 A_0 v_{12} &= -\beta_1\gamma_1 A_1 v_{11} - \beta_1\gamma_1 A_2 v_{10} - \beta_1 \partial_s v_{10} \\ &\quad - \Phi_1^2 k_1(y)v_{10} + \Phi_2^2 k_2(y)v_{20} \ \ \text{in} \ \ Y_\varepsilon^w, \\ & v_{12} \ \ \text{Y-periodic in} \ \ y, \end{aligned} \tag{32}$$

$$\begin{aligned} (d_1\nabla_y v_{12}, \tilde{n}) &= -(d_1\nabla_x v_{11}, \tilde{n}) - (d_1\nabla_x v_{10}, n') - (d_1\nabla_y v_{11}, n') \\ &\quad - \frac{\Phi_3^2}{\gamma_1}\eta(v_{10}, v_{50}) \ \ \text{on} \ \ \Gamma_\varepsilon^{sw}, \end{aligned} \tag{33}$$

$$\begin{aligned} (d_1\nabla_y v_{12}, \tilde{n}) &= -(d_1\nabla_x v_{11}, \tilde{n}) - (d_1\nabla_x v_{10}, n') \\ &\quad - (d_1\nabla_y v_{11}, n') \ \ \text{on} \ \ \Gamma_\varepsilon^{wa}, \end{aligned} \tag{34}$$

where

$$A_2 := -\sum_{i,j=1}^3 \frac{\partial}{\partial x_i}\left(d_1^{ij}\frac{\partial}{\partial x_j}\right).$$

From (30), we obtain that v_{10} is independent of y. Since the elliptic equation for v_{11} [with right-hand side defined in terms of v_{10}] is linear, its solution can be represented via

$$v_{11}(x,y,t) := -\sum_{k=1}^3 \chi^k(x,y,t)\frac{\partial v_{10}(x,t)}{\partial x_k} + v_1(x,t),$$

where the functions $\chi^k(x,y,t)$ solve the cell problem(s) and are periodic w.r.t. y. In the rest of the paper, we do not point out anymore the dependence of χ^k on the parameter t. The exact expression of v_1 does

not matter much at this stage. Using the expression of v_{11}, we obtain following cell problems in the standard manner:

$$A_0\chi^k(x,y) = -\sum_{i=1}^{3}\frac{\partial}{\partial y_i}d_1^{ik}(y), \ k \in \{1,2,3\} \ \text{in} \ Y^w, \qquad (35)$$

$$\sum_{i,j,k=1}^{3}\frac{\partial v_{10}}{\partial x_k}[d_1^{ij}\frac{\partial\chi^k}{\partial y_j}\tilde{n}_i - d_1^{jk}\tilde{n}_j] = 0, \ \text{on} \ \Gamma^{sw},$$

$$\sum_{i,j,k=1}^{3}\frac{\partial v_{10}}{\partial x_k}[d_1^{ij}\frac{\partial\chi^k}{\partial y_j}\tilde{n}_i - d_1^{jk}\tilde{n}_j] = 0, \ \text{on} \ \Gamma^{wa}$$

Since the right-hand side of (35) integrated over Y is zero, this problem has a unique solution. Note also that

$$\beta_1\gamma_1 A_0 v_{12} = \beta_1\gamma_1[-\sum_{i,j,k=1}^{3}\frac{\partial v_{10}}{\partial x_k}\frac{\partial}{\partial y_i}(d_1^{ij}\frac{\partial\chi^k}{\partial x_j})$$

$$-\sum_{i,j,k=1}^{3}\frac{\partial^2 v_{10}}{\partial x_j\partial x_k}\frac{\partial}{\partial y_i}(d_1^{ij}\chi^k) + \sum_{i,j=1}^{3}\frac{\partial d_1^{ij}}{\partial y_i}\frac{\partial\tilde{v}_1}{\partial x_j}$$

$$-\sum_{i,j,k=1}^{3}d_1^{ij}\frac{\partial^2\chi^k}{\partial x_i\partial y_j}\frac{\partial v_{10}}{\partial x_k} - \sum_{i,j,k=1}^{3}d_1^{ij}\frac{\partial\chi^k}{\partial y_i}\frac{\partial^2 v_{10}}{\partial x_k\partial x_i}$$

$$+\sum_{i,k=1}^{3}d_1^{ik}\frac{\partial^2 v_{10}}{\partial x_k\partial x_i}] - \beta_1\partial_s v_{10} - \Phi_1^2 k_1(y)v_{10} + \Phi_2^2 k_2(y)v_{20}.$$

Moreover, we have

$$\beta_1\gamma_1(d_1\nabla_y v_{12},\tilde{n}) = \beta_1\gamma_1[\sum_{i,j,k=1}^{3}d_1^{ij}\frac{\partial v_{10}}{\partial x_k}\frac{\partial\chi^k}{\partial x_i}\tilde{n}_j$$

$$+\sum_{i,j,k=1}^{3}d_1^{ij}\frac{\partial^2 v_{10}}{\partial x_j\partial x_k}\chi^k\tilde{n}_j - \sum_{i,j=1}^{3}d_1^{ij}\frac{\partial v_{10}}{\partial x_i}n_j'$$

$$-\sum_{i,j=1}^{3}d_1^{ij}\frac{\partial\tilde{v}_1}{\partial x_i}\tilde{n}_j + \sum_{i,j,k=1}^{3}d_1^{ij}\frac{\partial\chi^k}{\partial x_i}\frac{\partial v_{10}}{\partial x_k}n_j'$$

$$-\frac{\Phi_3^2}{\gamma_1}\eta(v_{10},v_{50})]. \qquad (36)$$

Writing down the compatibility condition (see e.g. Lemma 2.1 in [26]), we get

$$\int_{Y_\varepsilon^w}[\beta_1\gamma_1\{\sum_{i,j,k=1}^{3}\frac{\partial v_{10}}{\partial x_k}\frac{\partial}{\partial y_i}(d_1^{ij}\frac{\partial\chi^k}{\partial x_j}) + \sum_{i,j,k=1}^{3}\frac{\partial^2 v_{10}}{\partial x_j\partial x_k}\frac{\partial}{\partial y_i}(d_1^{ij}\chi^k)$$

$$- \sum_{i,j=1}^{3} \partial d_1^{ij} \partial y_i \frac{\partial \tilde{v}_1}{\partial x_j} + \sum_{i,j,k=1}^{3} d_1^{ij} \frac{\partial^2 \chi^k}{\partial x_i \partial y_j} \frac{\partial v_{10}}{\partial x_k}$$

$$+ \sum_{i,j,k=1}^{3} d_1^{ij} \frac{\partial \chi^k}{\partial y_i} \frac{\partial^2 v_{10}}{\partial x_k \partial x_i} - \sum_{i,j,k=1}^{3} d_1^{ij} \frac{\partial^2 v_{10}}{\partial x_j \partial x_i} \}$$

$$+ \beta_1 \partial_s v_{10} + \Phi_1^2 k_1(y) v_{10} - \Phi_2^2 k_2(y) v_{20}] dy$$

$$= \beta_1 \gamma_1 \int_{\Gamma^{sw}} [\sum_{i,j,k=1}^{3} d_1^{ij} \frac{\partial v_{10}}{\partial x_k} \frac{\partial \chi^k}{\partial x_i} \tilde{n}_j$$

$$+ \int_{\Gamma^{sw}} \left[\sum_{i,j,k=1}^{3} d_1^{ij} \frac{\partial^2 v_{10}}{\partial x_j \partial x_k} \chi^k \tilde{n}_j - \sum_{i,j=1}^{3} d_1^{ij} \frac{\partial v_{10}}{\partial x_i} n_j' \right] d\sigma$$

$$- \int_{\Gamma^{sw}} \left[\sum_{i,j=1}^{3} d_1^{ij} \frac{\partial \tilde{v}_1}{\partial x_i} \tilde{n}_j + \sum_{i,j,k=1}^{3} d_1^{ij} \frac{\partial \chi^k}{\partial x_i} \frac{\partial v_{10}}{\partial x_k} n_j' \right] d\sigma_y$$

$$- \int_{\Gamma^{sw}} \frac{\Phi_3^2}{\gamma_1} \eta(v_{10}, v_{50})] d\sigma_y. \tag{37}$$

We apply Stokes' theorem to the terms involving $\tilde{n}_j$ and after straightforward calculations, we obtain

$$\beta_1 \partial_s v_{10} + \Phi_1^2 v_{10} \frac{1}{|Y_\varepsilon^w|} \int_{Y_\varepsilon^w} k_1(y) dy - \Phi_2^2 v_{20} \frac{1}{|Y_\varepsilon^w|} \int_{Y_\varepsilon^w} k_2(y) dy$$

$$- \beta_1 \gamma_1 \sum_{i,j,k=1}^{3} \frac{\partial^2 v_{10}}{\partial x_i \partial x_k} \langle d_1^{ij} \frac{\partial \chi^k}{\partial y_j} - d_1^{ik} \rangle$$

$$- \beta_1 \gamma_1 \sum_{i,j,k=1}^{3} \langle d_1^{ij} \frac{\partial^2 \chi^k}{\partial x_i \partial y_j} \rangle \frac{\partial v_{10}}{\partial x_k}$$

$$= -\beta_1 \gamma_1 \sum_{i,j,k=1}^{3} \frac{\partial v_{10}}{\partial x_k} \frac{1}{|Y_\varepsilon^w|} \int_{\Gamma_\varepsilon^{sw}} (d_1^{kj} n_j' - d_1^{ij} \frac{\partial \chi^k}{\partial y_i n_j'}) d\sigma_y$$

$$- \frac{\beta_1 \gamma_1}{\gamma_1} \Phi_3^2 v_{10} \frac{1}{|Y_\varepsilon^w|} \int_{\Gamma_\varepsilon^{sw}} v_{50}(x, y, t) k_3(y) d\sigma_y, \tag{38}$$

where $\langle f \rangle_V := \frac{1}{V} \int_V f dx$ for any V a subset of either Y_ε^a or Y_ε^w. The latter PDE can be rewritten as

$$\beta_1 \partial_s v_{10} - \beta_1 \gamma_1 \sum_{i,j,k=1}^{3} \frac{\partial}{\partial x_i} (\langle d_1^{ij} \frac{\partial \chi^k}{\partial y_j} - d_1^{ik} \rangle \frac{\partial v_{10}}{\partial x_k}) + \Phi_1^2 v_{10} K_1 - \Phi_2^2 v_{20} K_2$$

$$= -\beta_1 \gamma_1 \sum_{k=1}^{3} \frac{\partial v_{10}}{\partial x_k} U_k - \beta_1 \Phi_3^2 v_{10} K_3 \quad \text{in } \Omega, \tag{39}$$

and $v_{10} = 0$ on Γ, where

$$K_\ell \; := \; \frac{1}{|Y_\varepsilon^w|} \int_{Y_\varepsilon^w} k_\ell(y)dy, \; \ell \in \{1, 2\} \tag{40}$$

$$K_3 \; := \; \frac{1}{|Y_\varepsilon^w|} \int_{\Gamma_\varepsilon^{sw}} v_{50}(x, y, t)k_3(y)d\sigma_y, \tag{41}$$

and

$$U_k := \frac{1}{|Y_\varepsilon^w|} \sum_{i,j=1}^{3} \int_{\Gamma_\varepsilon^{sw}} (d_1^{kj} n_j' - d_1^{ij} \frac{\partial \chi^k}{\partial y_i} n_j')d\sigma_y. \tag{42}$$

The terms U_k are new. They occur due to the assumed deviation from a uniformly periodic distribution of perforations.

Now we apply the same procedure to the next mass-balance equation. To do this, we consider the auxiliary cell problem

$$\begin{aligned} A_0\chi^k(x,y) &= -\sum_{i=1}^{3} \frac{\partial}{\partial y_i} d_2^{ik}(y), \; k \in \{1, 2, 3\} \text{ in } Y^w, \\ \sum_{i,j,k=1}^{3} \frac{\partial v_{10}}{\partial x_k}[d_1^{ij} \frac{\partial \chi^k}{\partial y_j} \tilde{n}_i - d_1^{jk} \tilde{n}_j] &= 0, \text{ on } \Gamma^{sw}, \\ \sum_{i,j,k=1}^{3} \frac{\partial v_{10}}{\partial x_k}[d_1^{ij} \frac{\partial \chi^k}{\partial y_j} \tilde{n}_i - d_1^{jk} \tilde{n}_j] &= 0, \text{ on } \Gamma^{wa}, \end{aligned} \tag{43}$$

whose solution is $\chi^k(x, y)$. We obtain the upscaled PDE:

$$\beta_2 \partial_s v_{20} \; - \; \Phi_1^2 v_{10} k_1 + \Phi_2^2 v_{20} k_2 - \beta_2 \gamma_2 \sum_{i,j,k=1}^{3} \frac{\partial}{\partial x_i}(\langle d_2^{ij} \frac{\partial \chi^k}{\partial y_j} - d_2^{ik}\rangle \frac{\partial v_{20}}{\partial x_k}) =$$

$$- \; \beta_2 \gamma_2 \sum_{k=1}^{3} \frac{\partial v_{20}}{\partial x_k} U_k - \beta_3 Bi_M v_{30} C + \beta_2 Bi^M v_{20} B, \tag{44}$$

holding in Ω and

$$v_{20} = 0 \text{ on } \Gamma,$$

where

$$C \; := \; \frac{1}{|Y_\varepsilon^w|} \int_{\Gamma_\varepsilon^{wa}} b(y)H(y)d\sigma_y, \tag{45}$$

$$H(\frac{x}{\varepsilon}) \; := \; \frac{a_\varepsilon(x)}{b_\varepsilon(x)} \tag{46}$$

$$B \; := \; \frac{1}{|Y_\varepsilon^w|} \int_{\Gamma_\varepsilon^{wa}} b(y)d\sigma_y, \tag{47}$$

$$U_k \; := \; \frac{1}{|Y_\varepsilon^w|} \sum_{i,j=1}^{3} \int_{\Gamma_\varepsilon^{wa}} (d_1^{kj} n_j' - d_1^{ij} \frac{\partial \chi^k}{\partial y_i} n_j')d\sigma_y. \tag{48}$$

We treat now the mass-balance equation for $H_2S(g)$. The corresponding cell problems are given by

$$A_0 \chi^k(x,y) = -\sum_{i=1}^3 \frac{\partial}{\partial y_i} d_3^{ik}(y), \ k=1,2,3 \ \text{in} \ Y^a,$$
$$\sum_{j,k=1}^3 \frac{\partial v_{30}}{\partial x_k} [\sum_{i=1}^3 d_3^{ij} \frac{\partial \chi^k}{\partial y_j} \tilde{n}_i - d_3^{jk} \tilde{n}_j] = 0 \ \text{on} \ \Gamma^{wa},$$
$$\sum_{j,k=1}^3 \frac{\partial v_{30}}{\partial x_k} [\sum_{i=1}^3 d_3^{ij} \frac{\partial \chi^k}{\partial y_j} \tilde{n}_i - d_3^{jk} \tilde{n}_j] = 0 \ \text{on} \ \Gamma^{wa},$$

while the macroscopic PDE is

$$\partial_s v_{30} \ - \ \sum_{i,j,k=1}^3 \frac{\partial}{\partial x_i} (\langle d_3^{ij} \frac{\partial \chi^k}{\partial y_j} - d_3^{ik} \rangle \frac{\partial v_{30}}{\partial x_k})$$
$$= -\sum_{k=1}^3 \frac{\partial v_{30}}{\partial x_k} U_k + \beta_3 Bi_M v_{30} C - \beta_2 Bi_M v_{20} B \qquad (49)$$

in Ω with $v_{30} = v_{30}^D$, on Γ^D. Here we have

$$C \ := \ \frac{1}{|Y_\varepsilon^a|} \int_{\Gamma_\varepsilon^{wa}} b(y) H(y) d\sigma_y, \qquad (50)$$

$$B \ := \ \frac{1}{|Y_\varepsilon^a|} \int_{\Gamma_\varepsilon^{wa}} b(y) d\sigma_y. \qquad (51)$$

Same procedure leads to

$$\beta_4 \partial_s v_{40} \ - \ \Phi_1^2 v_{10} k_1 - \beta_4 \gamma_4 \sum_{i,j,k=1}^3 \frac{\partial}{\partial x_i} (\langle d_4^{ij} \frac{\partial \chi^k}{\partial y_j} - d_4^{ik} \rangle \frac{\partial v_{40}}{\partial x_k})$$
$$= -\beta_4 \gamma_4 \sum_{k=1}^3 \frac{\partial v_{40}}{\partial x_k} U_k, \qquad (52)$$

in Ω with $v_{40} = 0$, on Γ.

Interestingly, the case of the ODE for gypsum

$$\partial_s v_5^\varepsilon \ = \ \Phi_3^2 \eta(v_1^\varepsilon, v_5^\varepsilon) \ \text{on} \ \Gamma_\varepsilon^{sw}, \ s \in S, \qquad (53)$$
$$v_5^\varepsilon(x,0) \ = \ v_{50}^\varepsilon(x), \qquad (54)$$

seems to be more problematic. Let us firstly use the same homogenization ansatz as before and employ

$$\tilde{\eta}(v_1^\varepsilon, v_5^\varepsilon) = \eta_0^A(v_{10}(x,t), v_{50}(x,y,t)) + \mathcal{O}(\varepsilon).$$

We obtain

$$\partial_s v_{50}(x,y,t) \ = \ \Phi_3^2 \eta_0^A(v_{10}(x,t), v_{50}(x,y,t)) \qquad (55)$$
$$v_{50}(x,y,0) \ = \ v_{50}(x,y), \qquad (56)$$

where $v_{50}(x, y, t)$ is periodic w.r.t y. Notice that we can not obtain an expression for $v_{50}(x, y, t)$ that is independent of y!

On the other hand, if we make another ansatz for v_5^ε, say

$$v_5^\varepsilon(x, t) = v_{50}(x, t) + \varepsilon v_{51}(x, y, t) + \varepsilon^2 v_{52}(x, y, t) + \dots, \qquad (57)$$

then

$$\tilde{\eta}(v_1^\varepsilon, v_5^\varepsilon) = \eta_0^B(v_{10}(x, t), v_{50}(x, t)) + \mathcal{O}(\varepsilon)$$

and we obtain an averaged ODE independent of y as given via

$$\partial_s v_{50}(x, t) = \Phi_3^2 \eta_0^B(v_{10}(x, t), v_{50}(x, t)). \qquad (58)$$

The advantage of the second choice is that it leads to the averaged reaction constant $\bar{k}_3 = \frac{1}{|\Gamma_\varepsilon^{sw}|} \int_{\Gamma_\varepsilon^{sw}} k_3(y) dy$, which is, in practice, much nicer than (58). Summarizing: We have to choose between (55) and (58), but which of the two averaged ODEs is the right one? Does the correctness of the answer to this question depend on the choice of the initial datum for v_{50}? We will address these issues[7] in a forthcoming analyis paper where we justify rigorously the asymptotic behavior indicated here.

4.2. CASE 2: $d_3^\varepsilon = \mathcal{O}(1)$ AND $d_i^\varepsilon = \mathcal{O}(\varepsilon^2)$ FOR ALL $i \in \{1, 2, 4\}$

In this section, we take into account the fact that the diffusion of H_2S is much faster within the air-part of the pores than within the pore water. Particularly, we assume that d_3^ε is of order of $\mathcal{O}(1)$, while $d_i^\varepsilon = \mathcal{O}(\varepsilon^2)$ for all $i \in \{1, 2, 4\}$. We expect from the literature that the latter assumption will lead to a two-scale model for which the micro- and macro-structure need to be resolved simultaneously; see e.g. [16, 12, 23].

Assume the initial data to be given by $v_i^\varepsilon(x, 0) = v_i^0(x, \frac{x}{\varepsilon})$, $i \in \{1, 2, 3, 4, 5\}$ with functions $v_i^0 : \Omega \times Y \times S \to \mathbb{R}$ being Y-periodic with respect to the second variable $y \in Y$. Assume also that $d_i^\varepsilon = \varepsilon^2 d_i^0$, for $i \in \{1, 2, 4\}$ and $d_3^\varepsilon = d_3^0$. We employ the same homogenization ansatz

$$v_i^\varepsilon(x, t) = w_{i0}(x, y, t) + \varepsilon w_{i1}(x, y, t) + \varepsilon^2 w_{i2}(x, y, t) + \dots \qquad (59)$$

for all $i \in \{1, 2, 3, 4, 5\}$. Using the same strategy as in section 4.1, we obtain

$$\beta_1 \partial_s w_{10}(x, y, t) \; - \; \beta_1 \gamma_1 \nabla_y \cdot (d_1^0 \nabla_y w_{10}(x, y, t))$$
$$= -k_1(y) w_{10}(x, y, t) + k_2(y) w_{20}(x, y, t) \qquad (60)$$

---

[7] We anticipate here a bit the answer to the latter question: Trusting [20], relation (55) can be proven rigorously via a two-scale convergence approach. However, we will see that under some additional conditions (55) *reduces* to (58).

on $\Omega \times Y^w \times S$. The boundary conditions become

$$\tilde{n}(x,y) \cdot (-d_1^0 \nabla_y w_{10}(x,y,t)) = 0 \text{ on } \Omega \times \Gamma^{wa} \times S, \quad (61)$$

$$\tilde{n}(x,y) \cdot (-d_1^0 \nabla_y w_{10}(x,y,t)) = -\frac{\Phi_3^2}{\gamma_3} k_3(y) w_{10}(x,y,t) w_{50}(x,y,t) \quad (62)$$

on $\Omega \times \Gamma^{sw} \times S$.
Similarly,

$$\beta_2 \partial_s w_{20}(x,y,t) \;-\; \beta_2 \gamma_2 \nabla_y \cdot (d_2^0 \nabla_y w_{20}(x,y,t))$$
$$= k_1(y) w_{10}(x,y,t) - k_2(y) w_{20}(x,y,t), \quad (63)$$

in $\Omega \times Y^w \times S$ while the boundary conditions take the form

$$\tilde{n}(x,y) \cdot (-d_2^0 \nabla_y w_{20}(x,y,t)) = 0 \text{ on } \Omega \times \Gamma^{sw} \times S, \quad (64)$$

$$\tilde{n}(x,y) \cdot (-d_2^0 \nabla_y w_{20}(x,y,t)) = Bi^M b(y) \times$$
$$\times [\frac{\beta_3}{\beta_2} H(y) w_{30}(x,y,t) - w_{20}(x,y,t)] \text{ on } \Omega \times \Gamma^{wa} \times S. \quad (65)$$

Since we consider $d_3^\varepsilon = d_3^0$, we obtain the same macroscopic PDE as in Case 1:

$$\partial_s w_{30}(x,t) \;-\; \sum_{i,j,k=1}^3 \frac{\partial}{\partial x_i} (\langle d_3^{ij} \frac{\partial \chi^k}{\partial y_j} - d_3^{ik} \rangle \frac{\partial w_{30}(x,t)}{\partial x_k})$$
$$= -\sum_{k=1}^3 \frac{\partial w_{30}(x,t)}{\partial x_k} U_k + \beta_3 Bi^M w_{30}(x,t) C - \beta_2 Bi^M w_{20}(x,t) B$$
$$(66)$$

in Ω and

$$w_{30}(x,t) = w_{30}^D(x,t) \text{ on } \Gamma^D,$$

where

$$C := \frac{1}{|Y_\varepsilon^w|} \int_{\Gamma_\varepsilon^{wa}} b(y) H(y) d\sigma_y, \quad (67)$$

$$B := \frac{1}{|Y_\varepsilon^w|} \int_{\Gamma_\varepsilon^{wa}} b(y) d\sigma_y, \quad (68)$$

$$U_k := \frac{1}{|Y_\varepsilon^w|} \sum_{i,j=1}^3 \int_{\Gamma_\varepsilon^{wa}} (d_1^{kj} n'_j - d_1^{ij} \frac{\partial \chi^k}{\partial y_i} n'_j) d\sigma_y. \quad (69)$$

Next, we have

$$\beta_4 \partial_s w_{40}(x,y,t) - \beta_4 \gamma_4 \nabla_y.(d_4^0 \nabla_y w_{40}(x,y,t)) = k_1(y) w_{10}(x,y,t), \quad (70)$$

on $\Omega \times Y^w \times S$, while the boundary conditions are now given by

$$\begin{aligned}
\tilde{n}(x,y) \cdot (-d_4^0 \nabla_y w_{40}(x,y,t)) = 0 \ \text{ on } \ \Omega \times \Gamma^{wa} \times S, \\
\tilde{n}(x,y) \cdot (-d_4^0 \nabla_y w_{40}(x,y,t)) = 0 \ \text{ on } \ \Omega \times \Gamma^{sw} \times S.
\end{aligned} \tag{71}$$

The ODE modeling gypsum growth takes the form

$$\beta_5 \partial_s w_{50}(x,y,t) = -\Phi_3^2 \eta(w_{10}(x,y,t) w_{50}(x,y,t)) \tag{72}$$

on $\Omega \times \Gamma^{sw} \times S$.

Acknowledgements

References

1. Agreba-Driolett, D., F. Diele, and R. Natalini: 2004, 'A mathematical model for the SO_2 aggression to calcium carbonate stones: Numerical approximation and asymptotic analysis'. *SIAM J. Appl. Math.* **64**(5), 1636–1667.
2. Auriault, J.-L.: 1991, 'Heterogeneous Medium: Is an Equivalent Macroscopic Description Possible?'. *Int. J. Eng. Sci.* **29**(7), 785–795.
3. Beddoe, R. E.: 2009, 'Modelling the evolution of damage to concrete by acid attack'. In: L. Franke (ed.): *Simulation of Time Dependent Degradation of Porous Materials: Final Report on Priority Program 1122.* Göttingen: Cuvillier Verlag, pp. 275–293.
4. Beddoe, R. E. and H. W. Dorner: 2005, 'Modelling acid attack on concrete: Part 1. The essential mechanisms'. *Cement and Concrte Reseacrch* **35**, 2333–2339.
5. Belyaev, A. G., A. L. Pyatnitskii, and G. A. Chechkin: 1998, 'Asymptotic behaviour of a solution to a boundary value problem in a perforated domain with oscillating boundary'. *Siberian Mathematical Journal* **39**(4), 621–644.
6. Bensoussan, A., J. L. Lions, and G. Papanicolau: 1978, *Asymptotic Analysis for Periodic Structures.* Amsterdam: North-Holland.
7. Böhm, M., F. Jahani, J. Devinny, and G. Rosen: 1998, 'A moving-boundary system modeling corrosion of sewer pipes'. *Appl. Math. Comput.* **92**, 247–269.
8. Chechkin, G. and A. L. Pianitski: 1999, 'Homogenization of boundary-value problem in a locally periodic perforated domain'. *Applicable Analysis* **71**(1), 215–235.
9. Chechkin, G. A. and T. P. Chechkina: 2004, 'On homogenization of problems in domains of the "infusorium" type'. *J. Math. Sci* **120**(3), 386–407.
10. Chechkin, G. A., A. L. Piatnitski, and A. S. Shamaev: 2007, *Homogenization. Methods and Applications*, Vol. 234 of *Translations of Mathematical Monographs.* Providence, Rhode Island: AMS.
11. Cioranescu, D. and P. Donato: 1999, *An Introduction to Homogenization.* Oxford University Press, New York.

12. Eck, C.: 2004, 'Homogenization of a phase field model for binary mixtures'. *Multiscale Model. Simul.* **3**(1), 1–27.
13. Fatima, T. and A. Muntean: 2009, 'Well-posedness and two-scale convergence for a pore model describing sulfate corrosion'. *in preparation.*
14. Hewlett, P. C.: 1998, 'Lea's Chemistry of Cement and Concrete'. *Elsevier Butterworth-Heinemenn Linacre House, Jordan Hill, Oxford* pp. 327–328.
15. Hornung, U. and W. Jäger: 1991, 'Diffusion, convection, adsorption, and reaction of chemicals in porous media'. *J. Diff. Eqs.* **92**, 199–225.
16. Hornung, U., W. Jäger, and A. Mikelic: 1994, 'Reactive transport through an array of cells with semi-permeable membranes'. *RAIRO M2AN* **28**(1), 59–94.
17. Jahani, F., J. Devinny, F. Mansfeld, I. G. Rosen, Z. Sun, and C. Wang: 2001a, 'Investigations of sulfuric acid corrosion of the concrete, I: Modeling and chemical observations'. *J. Environ. Eng.* **127**(7), 572–579.
18. Jahani, F., J. Devinny, F. Mansfeld, I. G. Rosen, Z. Sun, and C. Wang: 2001b, 'Investigations of sulfuric acid corrosion of the concrete, II: Electrochemical and visual observations'. *J. Environ. Eng.* **127**(7), 580–584.
19. Marchand, J., E. Samson, Y. Maltais, R. J. Lee, and S. Sahu: 2002, 'Predicting the performance of concrete structures exposed to chemically aggressive environment-field validation'. *Materials and Structures* **35**, 623–631.
20. Marciniak-Czochra, A. and M. Ptashnyk: 2008, 'Derivation of a macroscopic receptor-based model using homogenization techniques'. *SIAM J. Math. Anal.* **40**(1), 215–237.
21. Mascarenhas, M. L.: 1995, 'Homogenization problems in locally periodic perforrated domains'. In: *Proc. of the International Conference in Asymptotic Methods for Elastic Structures*. Berlin. NY, pp. 141–149.
22. Meier, S. A.: 2008, 'Two-scale models for reactive transport and evolving microstructure'. Ph.D. thesis, University of Bremen, Germany.
23. Meier, S. A. and A. Muntean: 2009, 'A two-scale reaction-diffusion system with micro-cell reaction concentrated on a free boundary'. *Comptes Rendus Mécanique* **336**(6), 481–486.
24. Meier, S. A., M. A. Peter, A. Muntean, M. Böhm, and J. Kropp: 2007, 'A two-scale approach to concrete carbonation'. In: *Proceedings First International RILEM Workshop on Integral Service Life Modeling of Concrete Structures*. Guimaraes, Portugal, pp. 3–10.
25. Müllauer, W., R. E. Beddoe, and D. Heinz: 2009, 'Sulfate attack on concrete - Solution concentration and phase stability'. In: *Concrete in Aggressive Aqueous Environments, Performance, Testing and Modeling*. Toulouse, France, pp. 18 – 27.
26. Persson, L. E., L. Persson, N. Svanstedt, and J. Wyller: 1993, *The Homogenization Method*. Lund: Chartwell Bratt.
27. Song, H. W., H. J. Lim, V. Saraswathy, and T. H. Kim: 2007, 'A micro-mechanics based corrosion model for predicting the service life of reinforced concrete structures'. *Int. J. Elect. Sci.* **2**, 341–354.
28. Taylor, H. F. W.: 1990, *Cement Chemistry*. London: Academic Press.
29. Tixier, R., B. Mobasher, and M. Asce: 2003, 'Modeling of damage in cement-based materials subjected to external sulfate attack. I: Formulation'. *Journal of Materials in Civil Engineering* pp. 305–313.
30. van Duijn, C., A. Mikelic, I. S. Pop, and C. Rosier: 2008, *Mathematics in Chemical Kinetics and Engineering*, Chapt. Effective dispersion equations for reactive flows with dominant Peclet and Damkohler numbers, pp. 1–45. Academic Press.

31. van Noorden, T.: 2009, 'Crystal precipitation and dissolution in a porous medium: Effective equations and numerical experiments'. *Multiscale Modeling and Simulation* **7**(3), 1220–1236.

PREVIOUS PUBLICATIONS IN THIS SERIES:

Number	Author(s)	Title	Month
09-22	T. Aiki M.J.H. Anthonissen A. Muntean	On a one-dimensional shape-memory alloy model in its fast-temperature-activation limit	June '09
09-23	J. Portegies	Efimov trimers in a harmonic potential	July '09
09-24	M.J.H. Anthonissen J.H.M. ten Thije Boonkkamp	A compact high order finite volume scheme for advection-diffusion-reaction equations	August '09
09-25	A. Muntean M. Neuss-Radu	Analysis of a two-scale system for gas-liquid reactions with non-linear Henry-type transfer	August '09
09-26	T. Fatima N. Arab E.P. Zemskov A. Muntean	Homogenization of a reaction-diffusion system modeling sulfate corrosion in locally-periodic perforated domains	August '09